Subnanosecond magnetization dynamics measured by the second-harmonic magneto-optic Kerr effect

T. M. Crawford[a)] and T. J. Silva
Electromagnetic Technology Division, National Institute of Standards and Technology, Boulder, Colorado 80303

C. W. Teplin and C. T. Rogers
Condensed Matter Laboratory, Department of Physics, University of Colorado at Boulder, Boulder, Colorado 80309

(Received 15 October 1998; accepted for publication 5 April 1999)

We have measured the in-plane magnetization dynamics of $Ni_{81}Fe_{19}$ films using the surface- and interface-sensitive second-harmonic magneto-optic Kerr effect. The dynamical magnetization was measured on patterned $Ni_{81}Fe_{19}$ stripes as a function of an in-plane magnetic field applied parallel to the anisotropy axis. The excitation sources were 100 ps risetime magnetic field impulses and steps. The minimum magnetization switching times were <300 ps, and precessional free-induction decay was observed. The dynamics for both impulse and step excitation are fitted to the Landau–Lifshitz equation, yielding values for the anisotropy field, gyroscopic splitting factor, and damping. The local surface precessional frequency and anisotropy are different from the average bulk values, demonstrating that this technique possesses the necessary sensitivity to detect variations in localized surface and interface dynamics. [S0003-6951(99)00622-1]

Freeman and co-workers have studied magnetization dynamics in $Ni_{81}Fe_{19}$ via *linear* magneto-optics, using the magneto-optic Kerr effect (MOKE).[1] Freeman's pump-probe magneto-optic sampling uses a fast rise time magnetic field ''pump'' to excite the magnetization on a picosecond time scale and an ultrashort optical ''probe'' to sample the magnetization at an instant of time.[1]

For this study, we use this technique with second-harmonic (SH) magneto-optics, whereby a sample is illuminated with light at frequency f and generates light at $2f$. SHMOKE offers unique features that complement linear magneto-optical techniques. For thin $Ni_{81}Fe_{19}$ films, an intensity contrast of 60% has been demonstrated for SHMOKE in the p-transverse geometry.[2] Furthermore, SHMOKE has shown extreme sensitivity to M at surfaces and interfaces.[3]

We employ lithographically patterned, coplanar waveguides, with 0.5 mm center conductor widths, to create impulse and step magnetic field excitations for driving the magnetization. The impulse fields are created by current pulses from an InGaAs photodiode and are nominally 100 A/m (1.25 Oe) with 80 ps rise time and 100 ps full-width at half maximum (FWHM). The step fields are created with current steps from a pulse generator and are nominally 200 A/m (2.5 Oe), doubled to 400 A/m (5 Oe), with an electrical short placed immediately after the sample. The step rise time is about 100 ps, with a 10 ns duration. The sample is a 75-nm-thick $Ni_{81}Fe_{19}$ film 250 μm wide and 4 mm long. The $Ni_{81}Fe_{19}$ is deposited in a field, creating a uniaxial anisotropy H_k parallel to the long axis. The film is grown on 100 μm thick Si to minimize the distance between the sample and waveguide, and is placed on the waveguide center conductor, where the in-plane field is nearly uniform, with its long axis x parallel to the waveguide. The y direction is perpendicular to the waveguide direction; z is perpendicular to the surface. The SHMOKE measurements are performed in the p-transverse geometry using a Ti:sapphire laser and 50 fs optical pulses.[2]

Figure 1 shows *impulse* response for three longitudinal (in-plane, parallel to stripe direction) bias fields H_b. The measurements were acquired using a ~25 μm diam optical spot centered on the sample width. The signal was normalized to the saturation magnetization M_s by SHMOKE hysteresis loops acquired before and after measurement. The magnetization oscillates at a frequency which increases with bias field. The sample response time (10%–90%) ranges from 372 ps at $H_b = 160$ A/m (2 Oe) to 205 ps at $H_b = 2.6$ kA/m (32 Oe), consistent with the observed precessional frequency. Figure 2 displays the *step* response for three longitudinal bias fields. The magnetization again undergoes damped precessional motion, now about a nonzero M_y, due to the nonzero static (10 ns duration) field H_p caused by the field step. The response time decreases and frequency increases with bias field, from 500 ps at $H_b = 0$ to <300 ps at $H_b = 1200$ A/m (15 Oe). Figures 1–2 demonstrate that SHMOKE can measure gyromagnetic precessional effects in $Ni_{81}Fe_{19}$ films, and that the magnetization response time can be reduced by applying a bias field to increase the precessional frequency.

The solid lines in Figs. 1 and 2 are fits to solutions of the Landau–Lifshitz (LL) equation, which describes precessional (gyromagnetic) effects for thin ferromagnetic films where $M_s \gg H_k$ and $\lambda \ll \gamma\mu_0 M_s$ (Ref. 4)

$$\frac{d^2\phi}{dt^2} + \lambda \frac{d\phi}{dt} + \mu_0 \gamma^2 \frac{\partial E}{\partial \phi} = 0, \tag{1}$$

where μ_0 is the permeability of free space, ϕ is the in-plane magnetization angle, λ is the damping constant, γ is the gyromagnetic ratio, and E is the angle-dependent free energy

[a)]Present address: Seagate Research, PLP-II Suite 201, 1520 Penn Ave., Pittsburgh, PA 15222.

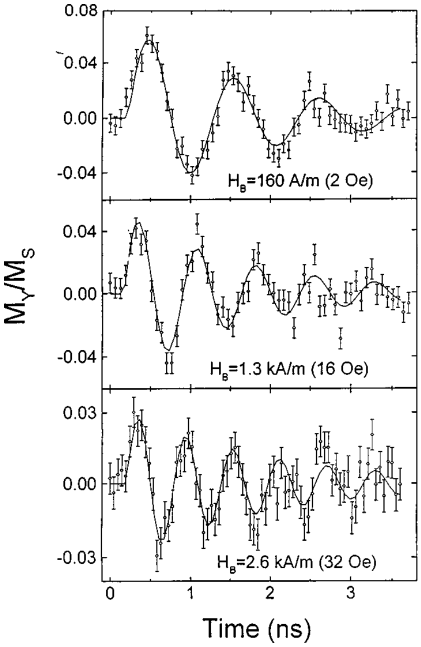

FIG. 1. Impulse magnetization response as a function of time for three different longitudinal bias fields: 0, 1.3 kA/m (16 Oe), and 2.6 kA/m (32 Oe). Amplitudes are normalized to the saturation SH intensity as determined by a static hard axis SHMOKE loop. The lines through the data are fits to Eq. (2). The data oscillate about $M_y = 0$, as is expected for the case of an impulse excitation.

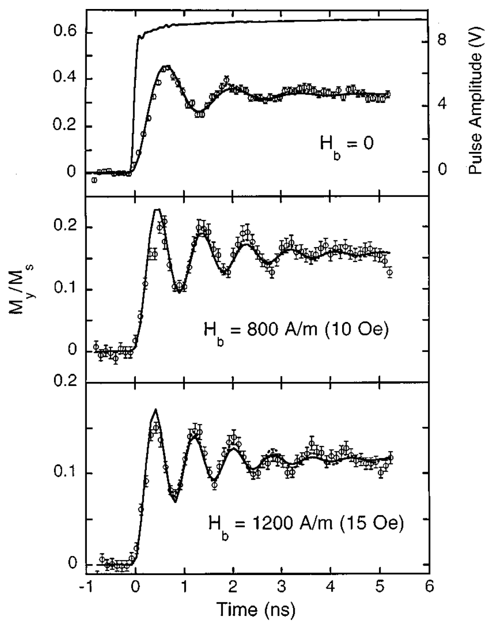

FIG. 2. Step magnetization response as a function of time for three different longitudinal bias fields: 0, 0.8 kA/m (10 Oe), and 1.2 kA/m (15 Oe). Amplitudes are normalized as in Fig. 1. As expected, M_y decreases with increasing H_b. The solid lines are numerical fits to Eq. (1), while the dashed lines are fits to Eq. (5). The top frame shows the measured, transmitted current waveform used as the drive function for the numerical fits.

density, which includes uniaxial anisotropy and Zeeman terms. In the limit of small excitations ($H_p \ll H_k$) and weak damping ($\lambda \ll \gamma\mu_0 M_s$), the LL solution is an exponentially damped sinusoid (DS)

$$\phi(t) = \frac{t_0 H_p \mu_0^2 \gamma^2 M_s}{\omega_p} [e^{-\lambda_i t/2} \sin(\omega_p t)], \tag{2}$$

where ω_p is the precession frequency, t_0 is the pulsed field duration (FWHM), and λ_i is the impulse damping parameter. The frequencies from Eq. (2) are shown in Fig. 3, and are well fitted by the Kittel equation for the case of small damping and impulse excitation[5]

$$f_p \approx \frac{\mu_0 \gamma}{2\pi} \sqrt{M_s(H_b + H_k)}. \tag{3}$$

We use a fixed value for $M_s = 813\,\text{kA/m}\,(\mu_0 M_s = 1\ \text{T})$, as measured with a superconducting quantum interference device magnetometer. The impulse start time is fitted and is $\sim$200 ps. A fit to Eq. (3) yields $H_k = 896 \pm 48\,\text{A/m}\,(11.2 \pm 0.6\,\text{Oe})$ and $\gamma = 25.2 \pm 0.3\,\text{GHz/T}$, or gyroscopic splitting factor $g \equiv \gamma h / 2\mu_B = 1.84 \pm 0.02$. We can extract H_p from the sinusoidal amplitude in Eq. (2), with the result $H_p = 73.6 \pm 16\,\text{A/m}\,(0.9 \pm 0.2\,\text{Oe})$. This value is in excellent agreement with the Karlqvist equation prediction for fields above a current stripe.[6]

For an ideal step excitation at $t = 0$, the solution to Eq. (1) in the small-signal, weak-damping limit is also a DS[7]

$$\phi(t) = \phi_0 [1 - \cos(\omega_p t) e^{-\lambda_s t/2}], \tag{4}$$

where ϕ_0 is the equilibrium offset angle, and λ_s is the step damping constant. Frequencies and offset angles are extracted from the time domain data by fitting the data in Fig. 2 with Eq. (4), for $t > 1.5$ ns. However, the fits are statistically poor. An improved fit can be obtained by fitting the data (dashed lines in Fig. 2) over the same time range with

$$\phi(t) = [\phi_0 - \phi' \cos(\omega_p t) e^{-\lambda_s t/2}], \tag{5}$$

where ϕ' is an additional fitting parameter which allows the sinusoidal precessional amplitude to vary independently of the equilibrium magnetization angle. While this expression is not valid at $t = 0$, where $\phi(t) = 0$, it is useful at times $>$1.5 ns because it significantly reduces the uncertainties in equilibrium angle and damping constant. The step precessional frequencies are shown in Fig. 3.

Ideally, ϕ_0 may be obtained by minimizing the free energy in the presence of H_k, H_p, and H_b, where H_p represents the field step (constant for $t \gg 0$), and H_b represents the bias field[4]

$$\left.\frac{\partial E}{\partial \phi}\right|_{\phi_0} = 0 = H_k \sin(\phi_0) - H_p(t) + H_b \tan(\phi_0). \tag{6}$$

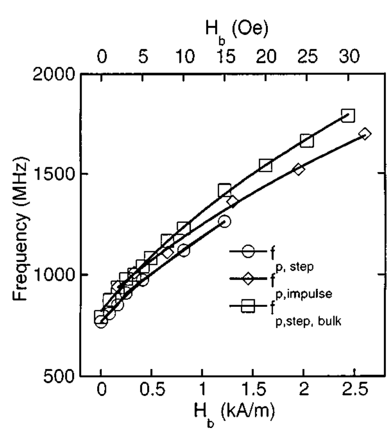

FIG. 3. Precessional frequencies for bulk, and SHMOKE step and impulse excitations as a function of longitudinal bias field with fits to Eqs. (3) and (7).

This expression can be used along with the Kittel formula for a step[7]

$$f_p \approx \frac{\mu_0 \gamma}{2\pi} \sqrt{M_s[H_p \sin(\phi_0) + H_b \cos(\phi_0) + H_k \cos(2\phi_0)]}, \tag{7}$$

to simultaneously fit the bias dependent values of ϕ_0 and f_p extracted from fitting the data to Eqs. (4) and (5). In this manner, we obtain values for g, H_p, and H_k. We again use $M_s = 813$ kA/m ($\mu_0 M = 1$ T). For the data shown in Fig. 2, we obtain $g = 1.72 \pm 0.04$, $H_k = 768 \pm 40$ A/m (9.6 ± 0.5 Oe), and $H_p = 242 \pm 20$ A/m (3.0 ± 0.25 Oe). We note that the fitted values of g, H_p, and H_k do not depend on whether Eqs. (4) or (5) is used to fit the data.

We also fitted the data in Fig. 2 using a full numerical solution to Eq. (1) (solid lines in Fig. 2), where we employ the voltage step measured after waveguide transmission as the drive function. These fits again yield values for g, H_k, and λ_s, and separate fits were performed for each bias field, allowing these parameters to vary independently. Again, the step starting time is fitted at ~200 ps. The mean parameter values for the different bias fields are $g = 1.89 \pm 0.08$, $H_k = 640 \pm 48$ A/m (8 ± 0.8 Oe), $H_p = 216 \pm 8$ A/m (2.7 ± 0.3 Oe), in partial agreement with the values obtained from fitting Eqs. (6) and (7).

The H_k obtained from both LL and DS fits agree and are slightly greater than the H_k obtained from fitting static SHMOKE hysteresis loops for these samples, for which $H_k = 550 \pm 40$ A/m (6.9 ± 0.5 Oe). The uniaxial anisotropy, measured using an $M-H$ looper on a co-deposited coupon, was 320 A/m (4 Oe). This result implies that there is additional anisotropy H_s which arises from shape effects, approximated by $H_s \approx 1.15 M_s \delta / w$, where δ is the film thickness and w is the sample width.[8] The fitted values of the damping constants λ_s [Eq. (5)] and λ_{DS} are shown in Table I. For the impulse measurements, λ_i is constant as a function of H_b, at $4 \times \pi \times 100 \pm 15$ MHz, $\lambda_s / 4\pi$ is also generally constant with H_b, but it increases at the lowest H_b. $\lambda_{DS}/4\pi$ is smaller than λ_s by ~30%, and is comparable to λ_i, at least for large H_b.

The impulse results in Fig. 1 are well fitted by the standard LL analysis, and the impulse and step results are generally in good agreement. However, the step case is more complicated. A close inspection of the data in Fig. 2 reveals that the solid curves slightly overshoot the first peak and undershoot subsequent peaks, while the dashed curves more closely reproduce the observed behavior. Fitting with Eq. (5) improves the value of chi-squared for the fit by 30%, reduces λ_{DS} by 30% and ϕ' by nearly 50%, compared with ϕ_0 at 1200 A/m (15 Oe) bias. Although Eq. (4) is an approximate solution to the LL equation, the fit to Eq. (4) is indistinguishable from the numerical fit, where Eq. (4) is derived assuming a perfect step function, and the numerical fit employs the measured step waveform with nonzero risetime and timing jitter. Therefore, the phenomenological inclusion of the extra parameter in Eq. (5) allows an improved fit which cannot be obtained by including risetime and jitter effects. Because the LL damping term predicts a precessional amplitude ϕ' which is equal to the switched magnetization angle ϕ_0 in the small-angle, weak-damping limit, we conclude that the step response data cannot be fully explained with a single-mode LL analysis. Further analytical progress will require a self-consistent modal analysis which properly accounts for the varying demagnetization energy across the width of the sample.[9]

TABLE I. Step excitation damping constants obtained via numerical integration of Eq. (1), λ_s, and via fitting with Eq. (5), λ_{DS}, as a function of bias field. The fits to Eq. (4) produce damping values similar to λ_s. The impulse damping λ_i was constant at $4 \times \pi \times 100 \pm 15$ MHz.

Bias field [A/m(Oe)]	$\lambda_s/4\times\pi$ (± 13 MHz)	$\lambda_{DS}/4\times\pi$ (± 17 MHz)
0	177	132
80 (1)	167	120
160 (2)	142	128
240 (3)	150	115
400 (5)	146	140
800 (10)	141	109
1200 (15)	150	97

In Eq. (7), $\gamma(g)$, and M_s are completely degenerate fitting parameters. Therefore, the data in Fig. 3 could easily be fitted to Eq. (7) with $M_s = 650$ kA/m ($\mu_0 M_s = 0.8$ T) and $g = 2.1$. In fact, measurements of the sample both by inductive time-domain measurements (Fig. 3) and ferromagnetic resonance (FMR), which are sensitive to the bulk value of M_s, yield $g = 2.1$ and $M_s = 813$ kA/m ($\mu_0 M = 1$ T).[10,11] To explain the surface behavior probed by SHMOKE, we require either a 20% reduction in M_s relative to the bulk value, a 10% reduction in g, or some combination of the two. Regardless, as shown in Fig. 3, the surface precessional frequencies are slower than those observed in the bulk.

A possible cause of a 20% reduction in M_s at the surface could be heating due to the intense laser beam incident on the sample. However, the equilibrium temperature of the film would have to be ~410 °C to reduce M_s by 20% for $Ni_{81}Fe_{19}$.[12] Previous annealing studies of similar $Ni_{81}Fe_{19}$ films with SHMOKE showed changes with annealing in air at 100 °C,[13] changes which are not observed here. Further measurements are needed to quantify this difference in surface and bulk frequencies.

[1] M. R. Freeman, A. Y. Elezzabi, and J. A. H. Stotz, J. Appl. Phys. **81**, 4516 (1997).
[2] T. M. Crawford, C. T. Rogers, T. J. Silva, and Y. K. Kim, Appl. Phys. Lett. **68**, 1573 (1996).
[3] J. Reif, J. C. Zink, C. M. Schneider, and J. Kirschner, Phys. Rev. Lett. **67**, 2878 (1991).
[4] D. O. Smith, J. Appl. Phys. **29**, 264 (1958).
[5] C. Kittel, *Introduction to Solid State Physics* (Wiley, New York, 1986).
[6] H. N. Bertram, *Theory of Magnetic Recording* (Cambridge University Press, Cambridge, 1994).
[7] T. J. Silva, C. S. Lee, T. M. Crawford, and C. T. Rogers, J. Appl. Phys. (in press).
[8] P. H. Bryant, J. F. Smyth, S. Schultz, and D. R. Fredkin, Phys. Rev. B **47**, 11255 (1993).
[9] G. M. Sandler, H. N. Bertram, T. J. Silva, and T. M. Crawford, J. Appl. Phys. **85**, 5080 (1999).
[10] T. J. Silva and T. M. Crawford, IEEE Trans. Magn. **35**, 671 (1999).
[11] C. Alexander, *MINT–University of Alabama* (1998).
[12] R. M. Bozorth, *Ferromagnetism* (IEEE, NJ, 1993).
[13] T. J. Silva, T. M. Crawford, C. T. Rogers, and Y. K. Kim, OSA Technical Digest Series **11**, 299 (1996).